Current Organic Chemistry, 2024, *28*, 230-240

RESEARCH ARTICLE

BENTHAM SCIENCE

Synthesis, Characterization, Molecular Docking Studies and Biological Evaluation of Some Novel 3,5-disubstituted-1-phenyl-4,5-dihydro-1*H*-pyrazole Derivatives

Fatih Tok[1,*], İlayda Rumeysa Bayrak[1], Elif Karakaraman[1], İrem Soysal[1], Cansel Çakır[2], Kübra Tuna[2], Serap Yılmaz Özgüven[3], Yusuf Sıcak[4], Mehmet Öztürk[2] and Bedia Koçyiğit-Kaymakçıoğlu[5]

[1]*Department of Pharmaceutical Chemistry, Faculty of Pharmacy, Marmara University, Istanbul, Türkiye;* [2]*Department of Chemistry, Faculty of Sciences, Muğla Sıtkı Koçman University, Muğla, Türkiye;* [3]*Department of Pharmaceutical Chemistry, Faculty of Pharmacy, Trakya University, Edirne, Türkiye;* [4]*Department of Medicinal and Aromatic Plants, Köyceğiz Vocational School, Muğla Sıtkı Koçman University, Muğla, Türkiye;* [5]*Department of Pharmaceutical Chemistry, Faculty of Pharmacy, Biruni University, Istanbul, Türkiye*

ARTICLE HISTORY

Received: November 10, 2023
Revised: December 20, 2023
Accepted: December 21, 2023

DOI:
10.2174/0113852728287379231229102847

Abstract: In this study, some new pyrazoline derivatives bearing cyano or nitro groups were synthesized. The structures of the compounds were characterized by IR, ^{1}H-NMR, ^{13}C-NMR and elemental analysis data. The ABTS$^{\cdot+}$, DPPH$^{\cdot}$, CUPRAC and β-Carotene/linoleic acid assays were carried out to determine the antioxidant activity of the synthesized pyrazolines. Compound **P14** showed higher antioxidant activity than the standard substance BHA with IC_{50} values of 1.71±0.31 µM and 0.29±0.04 µM in ABTS^{+} and β-carotene/linoleic acid assays, respectively. Compound **P12** also exhibited higher antioxidant activities than BHA with an IC_{50} value of 0.36±0.14 µM in β-carotene/linoleic acid analysis. In activity studies of pyrazolines against cholinesterase (AChE and BChE), tyrosinase, α-amylase and α-glucosidase, compound **P1** (IC_{50} = 39.51±3.80 µM) showed higher activity against α-amylase and compounds **P5** and **P12** displayed higher activity against α-glucosidase than acarbose with IC_{50} values of 14.09±0.62 and 83.26±2.57 µM, respectively. The drug-like properties such as Lipinski and Veber, bioavailability and toxicity risks of the synthesized compounds were also evaluated. The compounds were predicted to be compatible with Lipinski and Veber rules, have high bioavailability and low toxicity profiles. Moreover, molecular docking studies were performed to better understand the high activity of the compounds against a-amylase and a-glucosidase enzymes.

Fatih Tok

Keywords: Pyrazoline, molecular docking, antioxidant, α-amylase, α-glycosidase, toxicity.

1. INTRODUCTION

Pyrazoline structure is one of the important heterocyclic structures of pharmaceutical and medicinal chemistry [1]. They are preferred in a wide range of pharmacological activities such as antimicrobial, antidepressant, anticancer, anti-inflammatory, antioxidant and antidiabetic [2-5]. They can show various interactions, such as hydrogen bonding with enzymes and receptors, thus, they have an important place in the discovery of new drug-active ingredients [6]. Pyrazolines can also be used in various material sciences such as organic light-emitting diodes, optoelectronic devices and photographic conductor because of their good fluorescence appearance with good photostability [7]. Pyrazole and its derivative pyrazolines are widely found in nature in alkaloids, vitamins, pigments and plant and animal cell components [8]. Synthetically, pyrazolines are usually obtained in a two-step process. In the first step, the *α,β*-enone structure is obtained by the Claisen-Schmidt condensation reaction of acetophenone and aldehyde analogs [9]. In the second step, pyrazoline synthesis takes place from the cycloaddition reaction of this *α,β*-enone structure with hydrazine or diazoalkane structures [10]. Pyrazoline chemistry has been an active research area due to its biological and pharmaceutical properties, valuable physicochemical properties for sensor and optoelectronic applications, and their role as building blocks to achieve important structures [11]. As an example of the different biological effects of pyrazoline structures in our previous studies; we have reported that antipyrine derivatives carrying pyrazoline structure have strong AChE and MAO-B enzyme inhibitors, pyrazolines carrying benzo[d]thiazol-2(3H)-one structure have urease inhibitor, pyrazolines carrying benzodioxole structure exhibit strong anticancer activity [12-14]. Therefore, in continuation of our efforts to develop new pyrazolines, this article reports the synthesis of pyrazolines containing electron-withdrawing groups on the aromatic ring, such as cyano or nitro groups and the evaluation of their different biological effects, such as antioxidant, anticholinesterase, antityrosinase and antidiabetic.

2. RESULTS AND DISCUSSION

2.1. Chemistry

The synthesis of the target pyrazoline compounds was carried out in two steps. In the first step, chalcone derivatives were synthesized from 4-formylbenzonitrile or 4-nitroacetophenone compounds under Claisen-Schmidt condensation reaction conditions. In the

*Address correspondence to this author at the Department of Pharmaceutical Chemistry, Faculty of Pharmacy, Marmara University, Istanbul, Türkiye; Tel: +902167775200; E-mail: fatih.tok@marmara.edu.tr

1875-5348/24 $65.00+.00

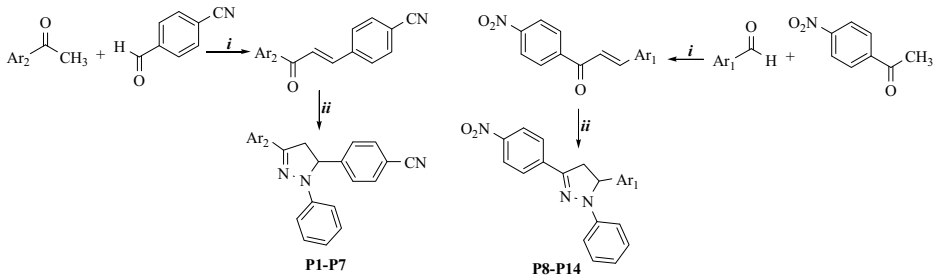

Scheme 1. The synthetic pathway of pyrazolines (**P1**-**P14**). Reagents and conditions: (**i**) Methanol, NaOH (10%, w/v), rt, 10 h; (**ii**) phenylhydrazine hydrochloride, ethanol, acetic acid, reflux, 6 h.

second step, pyrazoline derivatives (**P1**-**P14**) were obtained from chalcone compounds by ring closure under an acid-catalyzed process (Scheme **1**). IR, ^{1}H-NMR, ^{13}C-NMR spectroscopic methods and elemental analysis data were preferred to confirm the structures of the target compounds.

The most important band in the IR analysis of pyrazoline compounds (**P1**-**P14**) was C=N, which was sharply detected in the range of 1591-1599 cm^{-1}. Apart from this, characteristic C≡N stretching bands in the IR spectrum of cyano-bearing compounds (**P1**-**P7**) were observed in the range 2227-2229 cm^{-1}. Acharya *et al.* determined the stretching vibrations of the imine (C=N) group of the pyrazole compounds they synthesized in the range of 1592-1599 cm^{-1} [15].

In the ^{1}H-NMR analysis of the pyrazoline compounds (**P1**-**P14**), the most important clue indicating that the synthesis has taken place was the protons at the 4th and 5th positions of the pyrazoline ring observed in the range of 3.12-3.32 ppm, 3.93-4.03 ppm and 5.58-6.22 ppm in the form of three double doublets, respectively. Azarifar and Maleki reported that the protons at the 4th and 5th positions of the pyrazoline structure they synthesized similarly gave three doublets peaks in the ranges of 2.75-3.33, 3.12-4.11, 4.96-5.62 ppm, respectively. In addition, Maleki *et al.* indicated that the pyrazoline structure they synthesized gave three double doublet peaks at 3.05, 3.63 and 5.05 ppm [16, 17].

In the ^{13}C-NMR analysis of the pyrazoline structures (**P1**-**P14**), the carbons at the 3rd, 4th and 5th position of the pyrazolines were recorded as separate peaks in the range of 146.92-148.65 ppm, 42.33-43.78 ppm and 55.74-64.10 ppm, respectively. Al-Shammari *et al.* observed the imine carbon (C-3) at 156.64 ppm and the methylene carbon (C-4) at 38.45 ppm (Figs. **S1-43**) [18].

2.2. Biological Activity

The ABTS$^{\cdot+}$, DPPH·, CUPRAC and β-Carotene/linoleic acid assays were used to determine the antioxidant activities of the synthesized compounds. Antioxidant activity results are given in Table **1**. According to ABTS$^{\cdot+}$ assay results, **P14** carrying chlorine and nitro groups on the aromatic ring showed higher antioxidant activity than the standard substance BHA (IC_{50}=2.49±0.05 μM) with an IC_{50} value of 1.71-0.31 μM. Similarly, in β-Carotene/linoleic acid experiments, **P12** and **P14** carrying chlorine and nitro groups on the aromatic ring exhibited higher antioxidant activity than the standard substance BHA (IC_{50}=0.66±0.02 μM) with IC_{50} values of 0.36-0.14 μM and 0.29-0.04 μM, respectively.

Inhibition studies of the synthesized substances on enzymes responsible for different biological activities such as cholinesterase (AChE and BChE), tyrosinase, α-amylase and α-glucosidase were evaluated. The IC_{50} values of the compounds against these enzymes are given in Table **2**. The compounds showed no inhibitory activity against cholinesterase. Similarly, although the synthesized compounds showed inhibitory activity against tyrosinase, the effect was not as high as that of the standard compounds kojic acid and L-mimosine. However, significant results were obtained in α-amylase and α-glucosidase inhibition studies, which are important in terms of antidiabetic effect. **P1**, which carries cyano and methoxy groups on the aromatic ring, exhibited higher inhibitory activity against α-amylase enzyme than acarbose (IC_{50}=62.92±1.84 μM) with an IC_{50} value of 39.51±3.80 μM. On the other hand, compounds **P3**, **P5**, **P6**, **P7**, **P11** and **P12** showed higher inhibitory activity than acarbose (IC_{50} = 271.92±1.50 μM) with IC_{50} values of 14.09±0.62-268.77±0.60 μM against α-glucosidase. In fact, among these compounds, **P5** carrying chlorine and cyano group on the aromatic ring had the highest α-glucosidase inhibitory activity.

2.3. Molecular Docking Studies

Molecular docking analyses were performed using AutoDock Tools v.1.5.7 [19] to study the interactions between the synthesized compounds and α-amylase and α-glucosidase enzymes (PDB: 1B2Y and 5NN8, respectively). Compounds and target enzymes were prepared for docking, then the active amino acids in the binding sites were identified by determining the positioning of the active substances in enzymes as follows: α-amylase (PDB: 1B2Y), TRP59, TYR62, GLN63, THR163, LEU165, ARG195, ASP197, LYS200, HIS201, GLU233, GLU240, HIS299, ASP300, and HIS305; α-glucosidase (PDB: 5NN8) ASP282, TRP376, ASP404, TRP481, MET519, ARG600, ASP616, PHE649, and HIS674.

The binding energies calculated as a result of the docking process for all compounds are given in Table **3**.

Generally, docking studies were examined, and it was observed that the synthesized derivatives interacted with target enzymes through polar and nonpolar interactions are given in Table **3**. Docking analyses on α-amylase enzyme showed that compounds **P1** interacted with α-amylase with -8,4 kcal/mol binding energy. Compound **P1** interacts with THR163 *via* the *N* atom in the pyrazole ring and with the LYS200 *via* the *N* atom of the nitrile group *via* hydrogen bonding. The H atoms on the methoxy group interact with the amino acids TRP59 and TYR62 in the form of carbon-hydrogen interactions. It shows hydrophobic interactions with amino acids LEU162 and LEU165 (Fig. **1**).

As a result of the docking procedures performed on the α-glucosidase enzyme, it was found that compound **P5** interacted with the enzyme with a binding energy of -8.6 kcal/mol and compound **P12** with a binding energy of -8.3 kcal/mol. Compound **P5** was hydrogen bonded to amino acid ARG281 with N atom of nitrile group and showed hydrophobic pi interactions with amino acids ASP282, TRP481, TRP516, TRP613, ASP616, PHE649, and HIS674. Compound **P12** formed a hydrogen bond between the O

Table 1. Antioxidant activities of synthesized P1-P14[a].

Comp.	Ar_1/Ar_2	Antioxidant Activity			
		$ABTS^{\cdot+}$ Assay (IC_{50} µM)	DPPH· Assay (IC_{50} µM)	CUPRAC Assay ($A_{0.5}$ µM)	β-Carotene/Linoleic Acid Assay (IC_{50} µM)
P1	4-Methoxyphenyl	28.95±0.24	>400	113.59±0.01	23.70±0.69
P2	Thiophen-2-yl	55.66±0.96	>400	142.54±0.00	14.75±1.13
P3	5-Chlorothiophen-2-yl	31.05±2.21	329.60±0.64	150.20±0.02	19.52±0.85
P4	5-Bromothiophen-2-yl	21.74±0.63	239,92±0.31	148.56±0.04	92.89±1.10
P5	4-Chlorophenyl	24.92±1.29	372.37±0.30	168.08±0.00	33.99±0.85
P6	4-Fluorophenyl	31.93±1.66	>400	191.30±0.01	86.52±0.66
P7	*p*-Tolyl	43.42±0.28	>400	106.33±0.02	37.93±0.29
P8	3,4-Dichlorophenyl	84.28 ±2.03	299.08±1.97	60.94±0.01	5.43±0.11
P9	2,6-Dichlorophenyl	125.97±1.81	249.30±0.75	61.08±0.03	17.96±0.37
P10	*p*-Tolyl	NA	>400	60.14±0.00	15.01±0.21
P11	*m*-Tolyl	37.60±0.41	346.74±1.80	62.49±0.01	5.23±0.05
P12	4-Chlorophenyl	34.58±0.43	193.58±1.12	61.37±0.01	0.36±0.14
P13	2,6-Dimethylphenyl	>400	>400	56.96± 0.01	4.66±0.34
P14	3-Chlorophenyl	1.71 ±0.31	127.67±0.79	67.68±0.01	0.29±0.04
BHA[b]		2.49±0.05	5.93±0.20	5.74±0.41	0.66±0.02

Abbreviation: BHA, 2-tert-Butyl-4-hydroxyanisole.

Note: [a]Values expressed herein are mean ± SEM of three parallel measurements. $p<0.05$.
[NT]: not tested. [NA]: not active. [b]Reference compounds.

Table 2. Enzyme inhibition activities of synthesized P1-P14[a].

Comp.	Anticholinesterase Inhibition Activity		Tyrosinase Inhibition Activity IC_{50} (mM)	Antidiabetic Inhibition Activities	
	AChE Assay (IC_{50} µM)	BChE Assay (IC_{50} µM)		α-Amylase Inhibition Activity (IC_{50} µM)	α-Glucosidase Inhibition Activity (IC_{50} µM)
P1	NA	NA	NA	39.51 ± 3.80	NA
P2	NA	NA	153.48 ± 1.56	321.85 ± 14.32	NA
P3	NA	NA	>400	320.88 ± 2.71	179.76 ± 1.79
P4	NA	NA	326.95 ± 0.88	382.39 ± 26.38	NA
P5	NA	NA	35.91 ± 0.26	444.24 ± 25.69	14.09 ± 0.62
P6	NA	NA	150.61 ± 0.75	518.83 ± 31.47	245.15 ± 1.80
P7	NA	NA	NA	260.03 ± 7.89	201.49 ± 1.24
P8	NA	NA	20.40 ± 0.48	179.24 ± 0.42	316.96 ± 3.78
P9	NA	NA	20.56 ± 1.93	141.17 ± 3.33	290.87 ± 0.54
P10	NA	NA	16.26 ± 0.08	107.02 ± 1.63	NA
P11	NA	NA	21.09 ± 1.74	171.20 ± 5.09	268.77 ± 0.60
P12	NA	NA	21.07 ± 1.93	209.70 ± 6.73	83.26 ± 2.57
P13	NA	NA	13.27 ± 0.15	114.65 ± 4.36	NA
P14	NA	NA	90.48 ± 0.73	354.74 ± 13.47	NA
Galantaminb	1.82 ± 0.30	4.62 ± 0.12	NT	NT	NT
Kojic acidb	NT	NT	0.71 ± 0.54	NT	NT
L-mimosineb	NT	NT	0.79 ± 0.09	NT	NT
Acarboseb	NT	NT	NT	62.92 ± 1.84	271.92 ± 1.50

Note: [a] Values expressed herein are mean ± SEM of three parallel measurements. $p<0.05$.
[NT]: not tested. [NA]: not active. [b] Reference compounds.

Table 3. Enzyme inhibition activities of synthesized P1-P14[a].

Comp.	α-Amylase /PDB: 1B2Y		α-Glucosidase /PDB: 5NN8	
	Binding Energy (kcal/mol)	Interacted Amino Acids	Binding Energy (kcal/mol)	Interacted Amino Acids
P1	-8.4	TRP59[b], TYR62[b], LEU162[c], THR163[a], LEU165[c], LYS200[a]	-4.7	ASP404[b], TRP481[c], TRP516[c], ASP616[c], TRP618[a], LEU650[c], HIS674[c]
P2	-5.3	TYR62[c], LEU162[c], HIS201[b], HIS305[c]	-6.0	TRP481[c], MET519[c], ASP616[b], LEU650[c]
P3	-5.4	TYR62[c], LEU162[c], HIS201[b], HIS305[c]	-7.2	TRP481[c], TRP516[c], ASP616[c], PHE649[c], HIS674[c]
P4	-6.9	TPR59[c], LEU165[c], ARG195[a], HIS305[c], GLY306[b]	-5.4	ARG281[a], ASP282[c], ILE441[c], TRP481[c], MET519[c]
P5	-6.6	TPR58[c], TPR59[c], HIS299[c], HIS305[c]	-8.6	ARG281[a], ASP282[c], TRP481[c], TRP516[c], TRP613[c], ASP616[c], PHE649[c], HIS674[c]
P6	-5.7	TYR62[b], THR151[c], LEU162[c], LYS200[a], ILE235[c]	-7.1	ARG281[a], ASP282[d], LEU283[c], TRP481[c], ASP616[b]
P7	-6.1	TPR58[c], TPR59[c], TYR62[c]	-6.5	ARG281[a], ASP282[c], TRP481[c], MET519[c], HIS674[c]
P8	-7.9	TYR151[c], THR163[a], LYS200[a], ILE235[c], ALA307[c]	-6.7	ASP282[c], TRP481[c], ASP404[c], ASP518[c], MET519[c], HIS674[a]
P9	-6.4	TPR59[c], TYR62[c], LEU162[c], HIS305[c], ASP356[c]	-6.0	LEU283[c], ALA284[c], TRP481[c], PHE525[c], ASP616[c]
P10	-7.5	TPR58[c], TPR59[c], TYR62[c], ARG195[a,c,] ASP197[c,] HIS299[c], ASP300[c], HIS305[c]	-5.4	ASP404[c], TRP481[c], ASP518[c], PHE525[c], ARG600[c], ASP616[c] ARG672[c], HIS674[a]
P11	-7.0	TYR62[c], LEU162[c], ILE235[c], HIS305[c], GLY306[c], ALA307[c],	-7.4	ALA284[c], TRP376[c], TRP481[c], MET519[c], ASP616[c], PHE649[c], LEU650[c], LEU677[c]
P12	-6.1	TYR62[c], HIS299[c], HIS305[b,c]	-8.3	ASP282[c], ASP404[c], TRP481[c], ASP518[c], MET519[c], PHE525[c], HIS674[a]
P13	-7.7	TYR62[c], LEU162[c], LEU165[c], HIS305[c], ASP356[c]	-5.8	ASP404[c], ASP518[c], PHE525[c], ARG600[c], ASP616[c] ARG672[c], HIS674[a]
P14	-5.6	HIS101[c], LEU162[c], LEU165[c], LYS200[c], ILE235[c], HIS305[c]	-6.0	ASP404[c], TRP481[c], ASP518[c], MET519[c], PHE525[c], HIS674[a]
Acarbose	-9.1	TPR59[a,c], GLN63[a], TYR151[a], ASP197[a,b], ALA198[c], HIS201[a], GLU233[b], HIS299[a], ASP300[a], HIS305[c], GLY306[a,b]	-9.4	ASP282[a], ALA284[a], TRP376c, TRP481[c], ASP404[a,b], ASP518[b], ARG600[c], ASP616[c], PHE649[c], HIS674[a]

Note: a: H-bond b: C-H bond, c: Hydrophobic π-interaction, d: Halogen bond, e: Attractive charge.

atom of the nitro group and HIS674 and an attractive charge between the N atom and ASP4040 and ASP518. ASP282, TRP481, MET519 and PHE525 showed pi interactions with amino acids (Fig. **2**).

2.4. *In silico* ADME Studies

For a molecule with high biological activity to be a drug candidate, it must have acceptable physicochemical and pharmacokinetic properties [20]. Therefore, physicochemical and pharmacokinetic data of the synthesized pyrazolines were calculated and given in Table **4**. According to Lipinski's rule, at least three of the following four drug-like properties should be fulfilled; MW, logP, hydrogen bond acceptor and donor numbers should be less than 500, 5, 10 and 5, respectively [21]. Also, according to the Veber rule, the number of rotatable bonds and the total polar surface area should be less than 10 and 140, respectively [22]. Within the framework of these rules, all pyrazoline compounds (**P1**-**P14**) were in full compliance with both Lipinski and Veber rules. The bioavailability scores of the compounds were ideal and determined as 0.55.

For a molecule to be an oral drug candidate, it must easily pass through gastrointestinal membranes [23]. As a matter of fact, it is estimated that all synthesized pyrazolines (**P1**-**P14**) have high passage through gastrointestinal membranes. When the blood-brain barrier, another important physiological barrier, is considered, the passage of all compounds was expected to be high except for bulky groups carrying dichloro and nitro substituents on the aromatic ring, such as **P8** and **P9**. The BOILED-Egg model showed that all of the compounds except **P8** and **P9** can pass through gastrointestinal membranes and the blood-brain barrier because they are located in the yellow region (Fig. **3**). The compounds **P8** and **P9** are in the white region and can easily pass through gastrointestinal membranes.

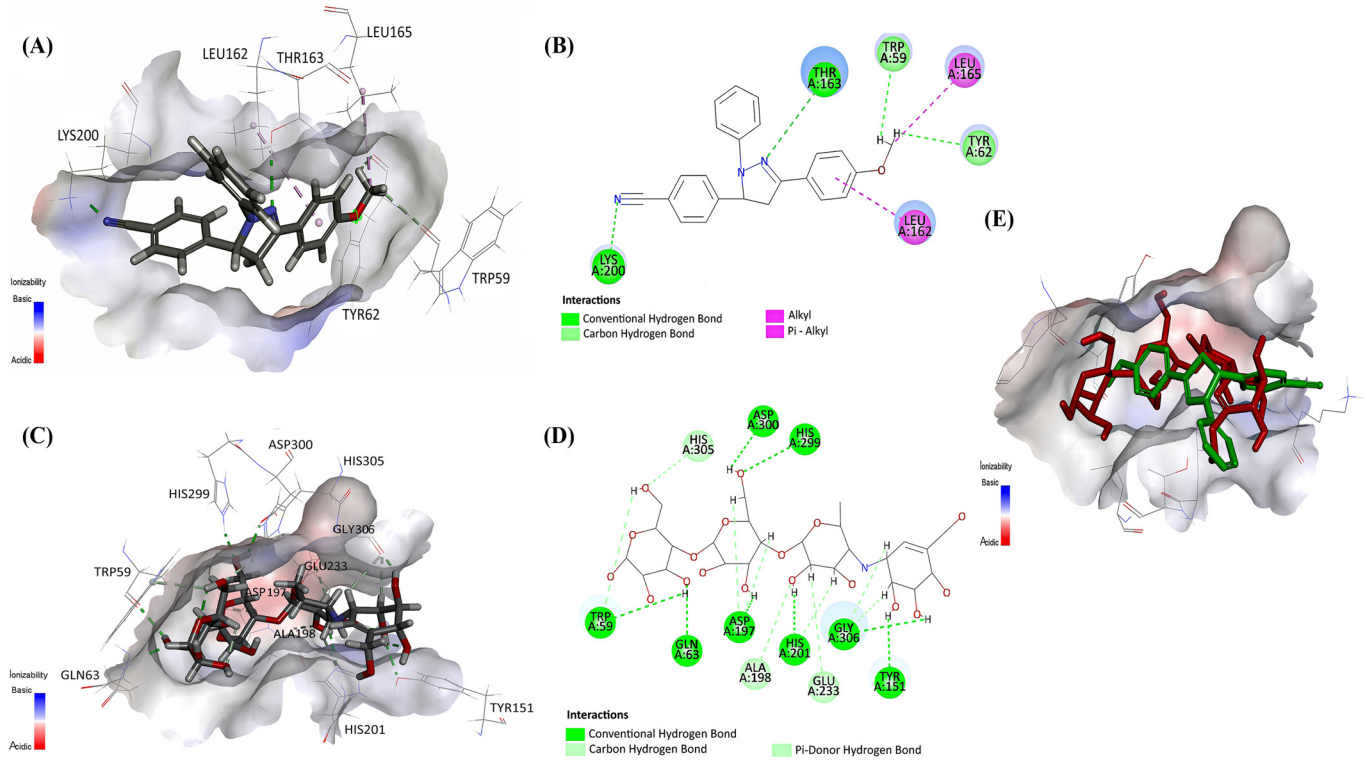

Fig. (1). (**A**) 3D interactions of **P1** with α-amylase (**B**) 2D interactions of **P1** with α-amylase (**C**) 3D interactions of acarbose with α-amylase (**D**) 2D interactions of acarbose with α-amylase (**E**) Overlaps of **P1** (green) and acarbose (red) in the binding site of α-amylase. *(A higher resolution / colour version of this figure is available in the electronic copy of the article).*

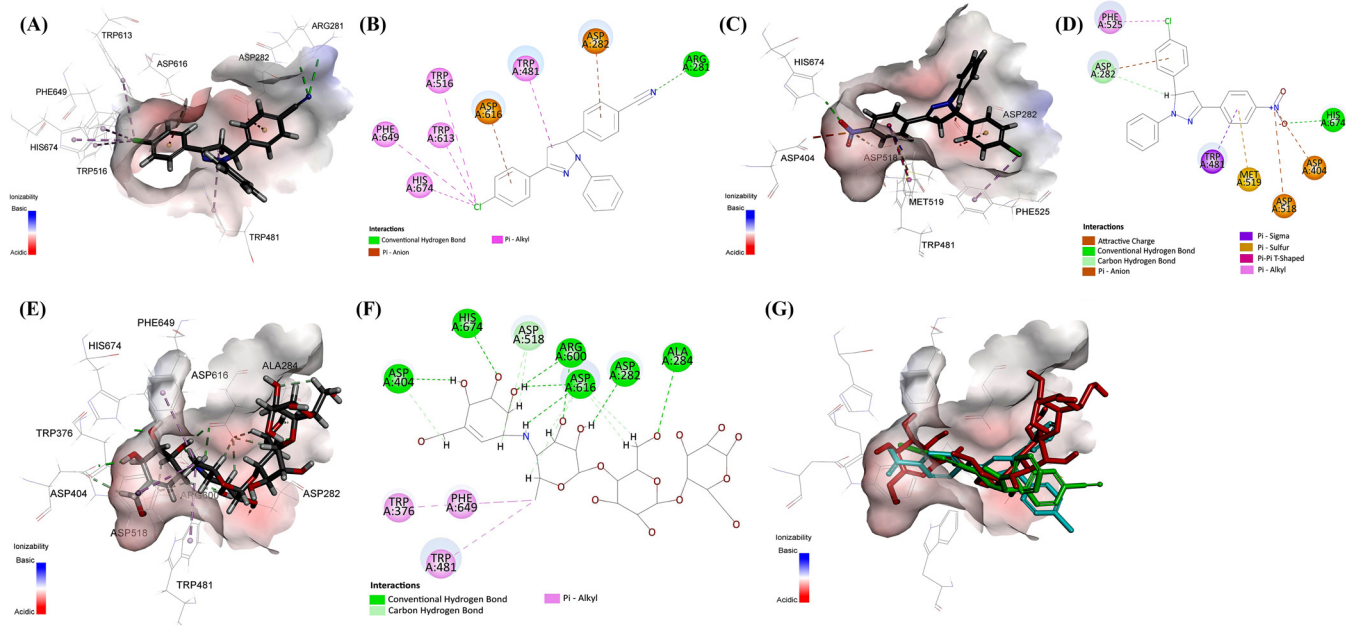

Fig. (2). (**A**) 3D interactions of **P5** with α-glucosidase (**B**) 2D interactions of **P5** with α-glucosidase (**C**) 3D interactions of **P12** with α-glucosidase (**D**) 2D interactions of **P12** with α-glucosidase (**E**) 3D interactions of acarbose with α-glucosidase (**D**) 2D interactions of acarbose with α-glucosidase (**E**) Overlaps of **P5** (green), **P12** (cyan) and acarbose (red) in binding site of α-glucosidase. *(A higher resolution / colour version of this figure is available in the electronic copy of the article).*

One of the important conditions for being a drug candidate is the assessment of toxicity risk [24]. As a matter of fact, the possible toxicity profiles of the synthesized pyrazolines are given in Table **5**. It is estimated that the compounds carrying nitro group on the aromatic ring (**P8**-**P14**) may have high mutagenic and reproductive effects, but not irritant and tumorigenic effects except **P13**. Compounds carrying cyano group on the aromatic ring (**P1**-**P7**) are not expected to have mutagenic, tumorigenic, reproductive and irritant risks.

Table 4. Physicochemical and pharmacokinetics of the pyrazolines.

Comp.	MW	mLogP	Num. H-bond Acceptors	Num. H-bond Donors	n-ROTB	TPSA	GI abs.	BBB per.	Bio. Score
P1	353.42	3.36	3	0	4	48.62	High	Yes	0.55
P2	329.42	3.32	2	0	3	67.63	High	Yes	0.55
P3	363.86	3.81	2	0	3	67.63	High	Yes	0.55
P4	408.31	3.92	2	0	3	67.63	High	Yes	0.55
P5	357.84	4.21	2	0	3	39.39	High	Yes	0.55
P6	341.38	4.11	3	0	3	39.39	High	Yes	0.55
P7	337.42	3.94	2	0	3	39.39	High	Yes	0.55
P8	412.27	4.28	3	0	4	61.42	High	No	0.55
P9	412.27	4.28	3	0	4	61.42	High	No	0.55
P10	357.41	3.53	3	0	4	61.42	High	Yes	0.55
P11	357.41	3.53	3	0	4	61.42	High	Yes	0.55
P12	377.82	3.80	3	0	4	61.42	High	Yes	0.55
P13	371.43	3.75	3	0	4	61.42	High	Yes	0.55
P14	377.82	3.80	3	0	4	61.42	High	Yes	0.55

Abbreviations: MW: Molecular weight, mlogP: partition coefficient, num. H-bond acceptors: number of hydrogen bond acceptors, num. H-bond donors: number of hydrogen bond donors, n-ROTB: number of rotatable bonds, TPSA: total polar surface area, GI abs.: gastrointestinal absorption, BBB per.: brain-blood barrier permeation, Bio. Score: Bioavailability score.

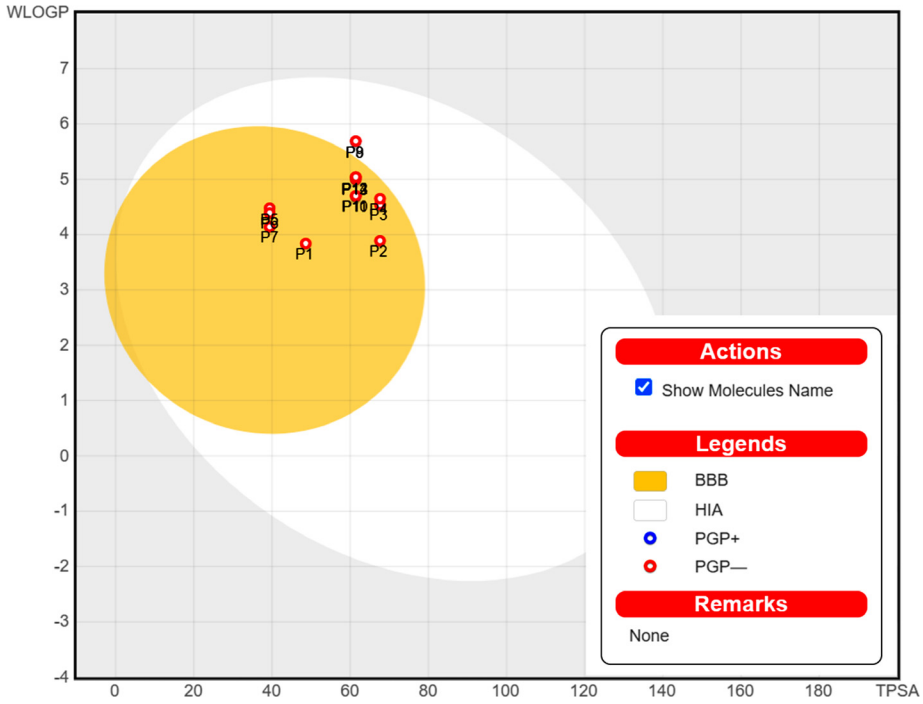

Fig. (3). The BOILED-Egg model of pyrazolines. *(A higher resolution / colour version of this figure is available in the electronic copy of the article).*

3. MATERIALS AND METHODS

3.1. Chemistry

All chemicals and solvents were purchased from Sigma-Aldrich (Sigma-Aldrich Corp., St. Louis, MO, USA). Thin layer chromatography (TLC) was used for monitoring reactions and chemical purities of the compounds. Melting points of pyrazolines were determined by Schmelzpunktbestimmer SMP II (Gottfried-Keller-Weg, Überlingen, Germany) and were uncorrected. Infrared spectra were recorded on a FTIR-8400S Shimadzu Spectrometer (Tokyo, Japan). ^{1}H-NMR and ^{13}C-NMR spectra were recorded in deuterated DMSO using Bruker Avance III HD 600 MHz spectrometer (Bruker Bioscience, Billerica, MA, USA) at 400 MHz for ^{1}H-NMR and 101 MHz for ^{13}C-NMR (decoupled), respectively. Elemental analyses were obtained using Leco CHNS-932.

3.1.1. The General Procedure of Chalcone Synthesis

1.0 mmol of Ketone derivatives [1-(4-methoxyphenyl)ethan-1-one: 0.15 g, 1-(thiophen-2-yl)ethan-1-one: 0.13 g, 1-(5-chlorothiophen-2-yl)ethan-1-one: 0.16 g, 1-(5-bromothiophen-2-yl)ethan-1-one: 0.21 g, 1-(4-chlorophenyl)ethan-1-one: 0.15 g, 1-(4-fluorophenyl)ethan-1-one: 0.14 g, 1-(p-tolyl)ethan-1-one: 0.13 g,

Table 5. The toxicity prediction of pyrazolines.

Comp.	Mutagenic	Tumorigenic	Reproductive Effective	Irritant
P1	None	None	None	None
P2	None	None	None	None
P3	None	None	None	None
P4	None	None	None	None
P5	None	None	None	None
P6	None	None	None	None
P7	None	None	None	None
P8	High	None	High	None
P9	High	None	High	None
P10	High	None	High	None
P11	High	None	High	None
P12	High	None	High	None
P13	High	None	High	High
P14	High	None	High	None

1-(4-nitrophenyl)ethan-1-one: 0.17 g] and 1.0 mmol of aldehyde derivatives [3,4-dichlorobenzaldehyde: 0.18 g, 2,6-dichlorobenzaldehyde: 0.18 g, 4-methylbenzaldehyde: 0.12 g, 3-methylbenzaldehyde: 0.12 g, 4-chlorobenzaldehyde: 0.14 g, 2,6-dimethylbenzaldehyde: 0.13 g, 3-chlorobenzaldehyde: 0.14 g, 4-formylbenzonitrile: 0.13 g] were dissolved in 15 mL of methanol at room temperature with stirring. Then 10% (w/v) NaOH (1 mL, 0.1 g) was added to the reaction medium. The mixture was stirred at room temperature for 10 h and terminated by TLC. The product obtained was washed with water and purified from ethanol [25].

3.1.2. The General Procedure of 2-pyrazoline Synthesis (P1-P14)

1.0 mmol of Chalcone derivatives [4-(3-(4-methoxyphenyl)-3-oxoprop-1-en-1-yl)benzonitrile: 0.26 g, 4-(3-oxo-3-(thiophen-2-yl)prop-1-en-1-yl)benzonitrile: 0.24 g, 4-(3-(5-chlorothiophen-2-yl)-3-oxoprop-1-en-1-yl)benzonitrile: 0.27 g, 4-(3-(5-bromothiophen-2-yl)-3-oxoprop-1-en-1-yl)benzonitrile: 0.32, 4-(3-(4-chlorophenyl)-3-oxoprop-1-en-1-yl)benzonitrile: 0.27 g, 4-(3-(4-fluorophenyl)-3-oxoprop-1-en-1-yl)benzonitrile: 0.25 g, 4-(3-(4-methylphenyl)-3-oxoprop-1-en-1-yl)benzonitrile: 0.25 g, 3-(3,4-dichlorophenyl)-1-(4-nitrophenyl)prop-2-en-1-one: 0.32 g, 3-(2,6-dichlorophenyl)-1-(4-nitrophenyl)prop-2-en-1-one: 0.32 g, 1-(4-nitrophenyl)-3-(*p*-tolyl)prop-2-en-1-one: 0.27 g, 1-(4-nitrophenyl)-3-(*m*-tolyl)prop-2-en-1-one: 0.27 g, 3-(4-chlorophenyl)-1-(4-nitrophenyl)prop-2-en-1-one: 0.29 g, 3-(2,6-dimethylphenyl)-1-(4-nitrophenyl)prop-2-en-1-one: 0.28 g, 3-(3-chlorophenyl)-1-(4-nitrophenyl)prop-2-en-1-one: 0.29 g] was dissolved in 15 mL ethanol by heating. Add 1.0 mmol phenylhydrazine hydrochloride (0.14 g) and 1.0 mL acetic acid to the solution. Then the mixture was heated in a water bath for 6 h. After checking by TLC, the excess solvent was evaporated and the solid was purified from ethanol [26].

Compounds **P1** (CAS number: 956222-22-3), **P7** (CAS number: 2587256-38-8) and **P10** (CAS number: 2906167-01-7) are included in the literature [27-29].

3.1.2.1. 4-(3-(4-Methoxyphenyl)-1-phenyl-4,5-dihydro-1H-pyrazol-5-yl)benzonitrile (P1)

Yellow solid, yield: 60%, m.p. = 145.2-146.0 ºC. IR (vmax, cm^{-1}): 3049 (=C-H), 2931, 2835, 2227 (C≡N), 1593 (C=N), 1516, 1496, 1455, 827. ^{1}H NMR (400 MHz, DMSO-d_6) δ 7.93 – 7.79 (m, 2H), 7.70 (ddt, *J* = 8.2, 5.2, 3.1 Hz, 2H), 7.58 – 7.41 (m, 2H), 7.16 (td, *J* = 7.8, 7.3, 3.7 Hz, 2H), 7.07 – 6.79 (m, 4H), 6.73 (dt, *J* = 8.2, 4.0 Hz, 1H), 5.58 (dd, *J* = 11.8, 5.9 Hz, 1H), 3.93 (ddd, *J* = 16.5, 12.3, 3.8 Hz, 1H), 3.80 (s, 3H), 3.13 (dd, *J* = 17.5, 5.6 Hz, 1H). ^{13}C NMR (101 MHz, DMSO-d_6) δ 160.43, 148.65 (C-3), 147.96, 144.70, 133.49, 129.47, 127.88, 127.53, 125.06, 119.14, 119.06, 114.62, 113.24, 110.68, 63.00 (C-5), 55.74 (OCH_3), 43.29 (C-4). Anal. calcd for $C_{23}H_{19}N_3O$: C, 78.16; H, 5.42; N, 11.89. Found: C, 77.42; H, 5.37; N, 11.99.

3.1.2.2. 4-(1-Phenyl-3-(thiophen-2-yl)-4,5-dihydro-1H-pyrazol-5-yl)benzonitrile (P2)

Orange solid, yield: 75%, m.p. = 168.8-170.0 ºC. IR (vmax, cm^{-1}): 3076 (=C-H), 2227 (C≡N), 1593 (C=N), 1496, 1444, 833. ^{1}H NMR (400 MHz, DMSO-d_6) δ 7.96 – 7.77 (m, 2H), 7.67- 7.36 (m, 4H), 7.24 – 7.03 (m, 3H), 6.92 (d, *J* = 8.2, 2H), 6.74 (t, *J* = 7.3, 1H), 5.63 (dd, *J* = 12.2, 6.1 Hz, 1H), 3.94 (dd, *J* = 17.3, 12.2, 1H), 3.16 (dd, *J* = 17.3, 6.1 Hz, 1H). ^{13}C NMR (101 MHz, DMSO-d_6) δ 148.17 (C-3), 144.36, 144.17, 135.76, 133.54, 129.54, 128.34, 128.32, 128.22, 127.51, 119.44, 119.11, 113.35, 110.80, 63.11 (C-5), 43.78 (C-4). Anal. calcd for $C_{20}H_{15}N_3S$: C, 72.92; H, 4.59; N, 12.76. Found: C, 73.30; H, 4.47; N, 12.83.

3.1.2.3. 4-(3-(5-Chlorothiophen-2-yl)-1-phenyl-4,5-dihydro-1H-pyrazol-5-yl)benzonitrile (P3)

Yellow solid, yield: 77%, m.p. = 90.5-91.0 ºC. IR (vmax, cm^{-1}): 3086 (=C-H), 2229 (C≡N), 1597 (C=N), 1498, 1471, 748. ^{1}H NMR (400 MHz, DMSO-d_6) δ 7.84 (dd, *J* = 8.4, 2.7 Hz, 2H), 7.53 – 7.36 (m, 2H), 7.29 – 6.96 (m, 4H), 6.91 (dd, *J* = 8.3, 2.7 Hz, 2H), 6.76 (td, *J* = 7.4, 2.6 Hz, 1H), 5.66 (ddd, *J* = 12.6, 6.3, 2.6 Hz, 1H), 3.93 (ddd, *J* = 17.6, 12.2, 2.8 Hz, 1H), 3.15 (ddd, *J* = 17.3, 6.2, 2.7 Hz, 1H). ^{13}C NMR (101 MHz, DMSO-d_6) δ 147.93 (C-3), 143.85, 143.65, 134.90, 133.57, 129.73, 129.57, 128.24, 127.85, 127.51, 119.72, 119.08, 113.43, 110.86, 63.21 (C-5), 43.06 (C-4). Anal. calcd for $C_{20}H_{14}ClN_3S$: C, 66.02; H, 3.88; N, 11.55. Found: C, 65.10; H, 3.90; N, 11.71.

3.1.2.4. 4-(3-(5-Bromothiophen-2-yl)-1-phenyl-4,5-dihydro-1H-pyrazol-5-yl)benzonitrile (P4)

Brown solid, yield: 68%, m.p. = 104.5-104.9 ºC. IR (vmax, cm^{-1}): 3093 (=C-H), 2227 (C≡N), 1597 (C=N), 1498, 1445, 748. ^{1}H NMR (400 MHz, DMSO-d_6) δ 7.91 – 7.65 (m, 3H), 7.31 – 7.00 (m,

5H), 6.96 – 6.67 (m, 3H), 5.66 (dd, *J* = 12.3, 6.2 Hz, 1H), 3.93 (dd, *J* = 17.5, 12.5 Hz, 1H), 3.13 (dd, *J* = 17.5, 6.2 Hz, 1H). ^{13}C NMR (101 MHz, DMSO-d_6) δ 147.93 (C-3), 143.85, 143.55, 137.51, 133.56, 132.41, 131.69, 129.57, 129.48, 128.70, 127.51, 119.71, 119.08, 113.46, 113.43, 113.16, 110.86, 63.21 (C-5), 43.13 (C-4). Anal. calcd for $C_{20}H_{14}BrN_3S$: C, 58.83; H, 3.46; N, 10.29. Found: C, 58.45; H, 3.40; N, 10.15.

3.1.2.5. 4-(3-(4-Chlorophenyl)-1-phenyl-4,5-dihydro-1H-pyrazol-5-yl)benzonitrile (P5)

Brown solid, yield: 80%, m.p. = 238.7-239.6 ºC. IR (vmax, cm^{-1}): 3059 (=C-H), 2229 (C≡N), 1599 (C=N), 1491, 1444, 829. ^{1}H NMR (400 MHz, DMSO-d_6) δ 7.80 (ddd, *J* = 29.3, 8.4, 1.8 Hz, 4H), 7.49 (ddd, *J* = 8.3, 4.0, 1.8 Hz, 5H), 7.17 – 6.88 (m, 3H), 6.76 (t, *J* = 7.2 Hz, 1H), 5.66 (dd, *J* = 12.5, 6.2 Hz, 1H), 3.95 (dd, *J* = 17.5, 12.5 Hz, 1H), 3.14 (dd, *J* = 17.5, 6.1 Hz, 1H). ^{13}C NMR (101 MHz, DMSO-d_6) δ 148.29 (C-3), 146.89, 144.15, 133.73, 133.53, 131.40, 129.53, 129.21, 127.93, 127.54, 119.60, 119.10, 113.46, 110.78, 63.19 (C-5), 42.86 (C-4). Anal. calcd for $C_{22}H_{16}ClN_3$: C, 73.84; H, 4.51; N, 11.74. Found: C, 73.53; H, 4.44; N, 11.89.

3.1.2.6. 4-(3-(4-Fluorophenyl)-1-phenyl-4,5-dihydro-1H-pyrazol-5-yl)benzonitrile (P6)

Yellow solid, yield: 75%, m.p. = 152.5-153.3 ºC. IR (vmax, cm^{-1}): 3066 (=C-H), 2227 (C≡N), 1597 (C=N), 1496, 1411, 831. ^{1}H NMR (400 MHz, DMSO-d_6) δ 7.89 – 6.93 (m, 12H), 6.74 (q, *J* = 7.4 Hz, 1H), 5.62 (dd, *J* = 12.4, 6.3 Hz, 1H), 3.93 (dd, *J* = 17.5, 12.0 Hz, 1H), 3.16 (dd, *J* = 17.5, 6.1 Hz, 1H). ^{13}C NMR (101 MHz, DMSO-d_6) δ 162.90, 148.41 (C-3), 147.13, 144.40, 133.52, 129.51, 128.48, 128.40, 127.54, 119.43, 119.11, 116.29, 116.07, 113.39, 110.76, 63.19 (C-5), 43.12 (C-4). Anal. calcd for $C_{22}H_{16}FN_3$: C, 77.40; H, 4.72; N, 12.31. Found: C, 76.77; H, 4.62; N, 12.37.

3.1.2.7. 4-(1-Phenyl-3-(p-tolyl)-4,5-dihydro-1H-pyrazol-5-yl)benzonitrile (P7)

Yellow solid, yield: 70%, m.p. = 173.7-174.5 ºC. IR (vmax, cm^{-1}): 3053 (=C-H), 2920, 2860, 2227 (C≡N), 1595 (C=N), 1498, 1454, 817. ^{1}H NMR (400 MHz, DMSO-d_6) δ 8.15 – 6.93 (m, 12H), 6.86 – 6.67 (m, 1H), 5.59 (dd, *J* = 12.5, 6.3 Hz, 1H), 3.93 (dd, *J* = 17.7, 12.3 Hz, 1H), 3.12 (dd, *J* = 17.7, 6.3 Hz, 1H), 2.34 (s, 3H). ^{13}C NMR (101 MHz, DMSO-d_6) δ 148.54 (C-3), 148.04, 144.52, 139.05, 133.50, 129.73, 129.49, 127.52, 126.27, 119.26, 119.12, 113.32, 110.70, 63.00 (C-5), 43.14 (C-4), 21.43 (CH_3). Anal. calcd for $C_{23}H_{19}N_3$: C, 81.87; H, 5.68; N, 12.45. Found: C, 81.44; H, 5.65; N, 12.50.

3.1.2.8. 5-(3,4-Dichlorophenyl)-3-(4-nitrophenyl)-1-phenyl-4,5-dihydro-1H-pyrazole (P8)

Brown solid, yield: 65%, m.p. = 116.7-117.2 ºC. IR (vmax, cm^{-1}): 3063 (=C-H), 1593 (C=N), 1550, 1498, 1455, 1319 (N=O), 848. ^{1}H NMR (400 MHz, DMSO-d_6) δ 8.42 – 8.10 (m, 2H), 8.10 – 7.77 (m, 2H), 7.72 – 7.50 (m, 2H), 7.31 – 7.12 (m, 3H), 7.12 – 6.98 (m, 2H), 6.83 (dd, *J* = 8.1, 6.6 Hz, 1H), 5.71 (dd, *J* = 12.6, 6.2 Hz, 1H), 3.98 (dd, *J* = 16.0, 12.0 Hz, 1H), 3.28 (dd, *J* = 16.0, 6.1 Hz, 1H). ^{13}C NMR (101 MHz, DMSO-d_6) δ 147.13 (C-3), 145.97, 143.44, 143.39, 138.90, 132.00, 131.85, 130.67, 129.66, 128.69, 126.93, 126.72, 124.46, 120.44, 113.91, 62.82 (C-5), 42.37 (C-4). Anal. calcd for $C_{21}H_{15}Cl_2N_3O_2$: C, 61.18; H, 3.67; N, 10.19. Found: C, 60.26; H, 3.59; N, 10.32.

3.1.2.9. 5-(2,6-Dichlorophenyl)-3-(4-nitrophenyl)-1-phenyl-4,5-dihydro-1H-pyrazole (P9)

Red solid, yield: 72%, m.p. = 185.0-185.4 ºC. IR (vmax, cm^{-1}): 3088 (=C-H), 1595 (C=N), 1555, 1496, 1435, 1336 (N=O), 850. ^{1}H NMR (400 MHz, DMSO-d_6) δ 8.32 – 8.13 (m, 2H), 7.98 (ddt, *J* = 6.8, 4.4, 2.0 Hz, 2H), 7.74 – 7.48 (m, 2H), 7.48 – 7.12 (m, 3H), 7.03 – 6.86 (m, 2H), 6.81 (q, *J* = 6.9, 6.0 Hz, 1H), 6.22 (dd, *J* = 12.0, 6.2 Hz, 1H), 4.01 (dd, *J* = 16.0, 12.0 Hz, 1H), 3.32 (dd, *J* = 11.9, 6.1 Hz, 1H). ^{13}C NMR (101 MHz, DMSO-d_6) δ 147.29 (C-3), 142.86, 138.73, 135.12, 131.41, 131.13, 129.63, 126.69, 124.55, 120.39, 113.40, 60.24 (C-5), 43.26 (C-4). Anal. calcd for $C_{21}H_{15}Cl_2N_3O_2$: C, 61.18; H, 3.67; N, 10.19. Found: C, 60.56; H, 3.72; N, 10.28.

3.1.2.10. 3-(4-Nitrophenyl)-1-phenyl-5-(p-tolyl)-4,5-dihydro-1H-pyrazole (P10)

Red solid, yield: 80%, m.p. = 148.5-149.2 ºC. IR (vmax, cm^{-1}): 3043 (=C-H), 1591 (C=N), 1550, 1500, 1455, 1315 (N=O), 844. ^{1}H NMR (400 MHz, DMSO-d_6) δ 8.39 – 8.15 (m, 2H), 8.08 – 7.82 (m, 2H), 7.26 – 7.00 (m, 8H), 6.79 (t, *J* = 7.3 Hz, 1H), 5.60 (dd, *J* = 12.6, 6.2 Hz, 1H), 3.94 (dd, *J* = 17.6, 12.5 Hz, 1H), 3.15 (dd, *J* = 17.6, 6.2 Hz, 1H), 2.25 (s, 3H). ^{13}C NMR (101 MHz, DMSO-d_6) δ 146.94 (C-3), 145.49, 143.64, 139.50, 139.21, 137.28, 130.09, 129.45, 126.71, 126.25, 124.45, 120.09, 113.94, 63.86 (C-5), 42.72 (C-4), 21.11 (CH_3). Anal. calcd for $C_{22}H_{19}N_3O_2$: C, 73.93; H, 5.36; N, 11.76. Found: C, 74.55; H, 5.37; N, 11.83.

3.1.2.11. 3-(4-Nitrophenyl)-1-phenyl-5-(m-tolyl)-4,5-dihydro-1H-pyrazole (P11)

Red solid, yield: 67%, m.p. = 133.6-133.9 ºC. IR (vmax, cm^{-1}): 3024 (=C-H), 2922, 2890, 1593 (C=N), 1552, 1498, 1455, 1336 (N=O), 844. ^{1}H NMR (400 MHz, DMSO-d_6) δ 8.34 – 8.18 (m, 2H), 8.10 – 7.89 (m, 2H), 7.29 – 7.12 (m, 5H), 7.07 – 6.64 (m, 4H), 5.60 (dd, *J* = 12.9, 6.4 Hz, 1H), 3.97 (dd, *J* = 17.7, 12.7 Hz, 1H), 3.18 (dd, *J* = 17.8, 6.2 Hz, 1H), 2.27 (s, 3H). ^{13}C NMR (101 MHz, DMSO-d_6) δ 146.96 (C-3), 145.54, 143.71, 142.60, 139.17, 138.82, 129.50, 129.47, 128.81, 126.77, 126.71, 124.47, 123.37, 120.13, 113.86, 64.10 (C-5), 42.82 (C-4), 21.56 (CH_3). Anal. calcd for $C_{22}H_{19}N_3O_2$: C, 73.93; H, 5.36; N, 11.76. Found: C, 74.77; H, 5.40; N, 11.59.

3.1.2.12. 5-(4-Chlorophenyl)-3-(4-nitrophenyl)-1-phenyl-4,5-dihydro-1H-pyrazole (P12)

Brown solid, yield: 65%, m.p. = 120.0-120.9 ºC. IR (vmax, cm^{-1}): 3064 (=C-H), 1593 (C=N), 1550, 1498, 1455, 1334 (N=O), 848. ^{1}H NMR (400 MHz, DMSO-d_6) δ 8.34 – 8.22 (m, 2H), 8.03 – 7.89 (m, 2H), 7.36 – 7.07 (m, 7H), 6.81 (t, *J* = 7.3 Hz, 2H), 5.70 (dd, *J* = 12.6, 6.1 Hz, 1H), 3.99 (dd, *J* = 17.6, 12.6 Hz, 1H), 3.21 (dd, *J* = 17.6, 6.1 Hz, 1H). ^{13}C NMR (101 MHz, DMSO-d_6) δ 147.05 (C-3), 145.69, 143.46, 141.38, 139.04, 132.60, 129.55, 128.35, 126.83, 126.22, 124.46, 120.27, 113.92, 63.29 (C-5), 42.53 (C-4). Anal. calcd for $C_{21}H_{16}ClN_3O_2$: C, 66.76; H, 4.27; N, 11.12. Found: C, 66.22; H, 4.31; N, 11.17.

3.1.2.13. 5-(2,6-Dimethylphenyl)-3-(4-nitrophenyl)-1-phenyl-4,5-dihydro-1H-pyrazole (P13)

Red solid, yield: 83%, m.p. = 182.2-183.0 ºC. IR (vmax, cm^{-1}): 3074 (=C-H), 2935, 1593 (C=N), 1550, 1498, 1455, 1313 (N=O), 844. ^{1}H NMR (400 MHz, DMSO-d_6) δ 8.39 – 8.06 (m, 2H), 8.06 – 7.79 (m, 2H), 7.14 (dtd, *J* = 20.8, 8.4, 7.4, 3.7 Hz, 4H), 7.00 – 6.86 (m, 3H), 6.79 (td, *J* = 7.3, 2.0 Hz, 1H), 5.81 (ddd, *J* = 13.2, 10.1, 2.2 Hz, 1H), 4.03 (ddd, *J* = 16.5, 13.9, 2.2 Hz, 1H), 3.15 (ddd, *J* = 17.8, 10.3, 2.2 Hz, 1H), 2.24 (s, 3H), 2.03 (s, 3H). ^{13}C NMR (101 MHz, DMSO-d_6) δ 146.92 (C-3), 145.76, 143.90, 139.12, 137.80, 136.16, 135.77, 131.02, 129.55, 129.26, 127.97, 127.91, 126.62, 124.51, 120.25, 113.30, 61.00 (C-5), 42.33 (C-4), 20.99 (CH_3), 19.55 (CH_3). Anal. calcd for $C_{23}H_{21}N_3O_2$: C, 74.37; H, 5.70; N, 11.31. Found: C, 74.77; H, 5.66; N, 11.38.

3.1.2.14. 5-(3-Chlorophenyl)-3-(4-nitrophenyl)-1-phenyl-4,5-dihydro-1H-pyrazole (P14)

Brown solid, yield: 73%, m.p. = 135.3-136.1 ºC. IR (vmax, cm^{-1}): 3068 (=C-H), 1593 (C=N), 1554, 1498, 1455, 1336 (N=O), 852. ^{1}H NMR (400 MHz, DMSO-d_6) δ 8.18 – 7.91 (m, 3H), 7.77 – 7.41 (m, 4H), 7.22 – 6.86 (m, 6H), 5.70 (dd, *J* = 12.8, 6.1 Hz, 1H), 3.98 (dd, *J* = 17.6, 12.7 Hz, 1H), 3.23 (dd, *J* = 17.9, 12.0 Hz, 1H). ^{13}C NMR (101 MHz, DMSO-d_6) δ 147.07 (C-3), 145.83, 144.91, 143.46, 139.83, 138.98, 134.02, 131.59, 130.98, 129.91, 129.46, 128.94, 126.89, 126.58, 125.06, 125.02, 124.47, 123.40, 120.33, 118.25, 113.03, 112.60, 63.33 (C-5), 42.54 (C-4). Anal. calcd for $C_{21}H_{16}ClN_3O_2$: C, 66.76; H, 4.27; N, 11.12. Found: C, 66.25; H, 4.33; N, 11.21.

3.1.3. Biological Activity

All biological activity measurements for **P1-P12** were using a 96-well microplate reader (Synergy H1 BioTek Multimode Reader). Value of activity experiments, which were performed in triplicate, 0.5 absorbances ($A_{0.5}$) for CUPRAC assay was calculated from the graph of bleaching rate (%) against sample concentrations, while all other assays were calculated as 50% inhibition activity (IC_{50}) with absorbance values against sample concentration. The DMSO was used as a negative control to follow the reaction.

3.1.4. In vitro Antioxidant Activity

The antioxidant activity performance of **P1-P14** derivatives was determined using the β-carotene bleaching method, DPPH free radical scavenging activity, ABTS cation radical scavenging activity, and cupric reducing antioxidant capacity (CUPRAC). The α-lpha-tocopherol (α-TOC) and butylatedhydroxytoluene (BHT) standards were used to compare the activity results.

3.1.4.1. Determination of ABTS Cation Radical Scavenging Activity of the P1-P14 Derivatives

The $ABTS^{\cdot+}$ scavenging activity was performed according to Re *et al.* (1999), with slight modifications [30-32]. Firstly, $ABTS^{\cdot+}$ solution was prepared by keeping 7 mM ABTS in water and 2.45 mM potassium persulfate at 20°C in the dark overnight. Before using the occurred $ABTS^{\cdot+}$ solution was made reading to get 0.35-0.4 ± 0.025 absorbance at 734 nm diluted 1:90 ration with EtOH. Then, 160 µL of prepared $ABTS^{\cdot+}$ reactive was mixed with 40 µL of **P1-P14** derivatives dissolved in DMSO at different concentrations. The absorbances of **P1-P14** for this assay were measured at 734 nm after 10 min incubation.

3.1.4.2. Determination of DPPH Free Radical Scavenging Activity of the P1-P14 Derivatives

The DPPH· scavenging activity was performed according to Blois (1958), with slight modifications. 160 µL of 0.004% of DPPH solution in EtOH was mixed with 40 µL of **P1-P14** derivatives dissolved in DMSO at different concentrations, 30 min incubation in the dark and the absorbance was measured at 517 nm [32, 33].

3.1.4.3. Determination of Cupric Reducing the Antioxidant Capacity of the P1-P14 Derivatives

Cupric reducing antioxidant capacity (CUPRAC) assay was performed according to Apak (2004). 50 µL of 10 mM Cu (II), 50 µL of 7.5 mM neocuproine, and 60 µL of NH_4Ac buffer (1 M, pH 7.0) were added to each well in a 96 well plate, respectively [32, 34]. To the mixture of each well in a 96, 40 µL of **P1-P14** derivatives at various concentrations were added, incubated for 1 h and absorbance was recorded at 450 nm.

3.1.4.4. Determination of the Lipid Peroxidation Inhibitory Activity of the P1-P14 Derivatives

The inhibitory activity of lipid peroxidation, which is based on the color change of β-carotene using a wavelength of 470 nm, the radical formed by lipid peroxidation from linoleic acid in water saturated with singlet oxygen, was evaluated using the β-carotene-linoleic acid assay [32, 35]. The more color exhibits more powerful lipid peroxidation inhibitor capacity. The reactive was prepared by mixing β-carotene (0.5 mg) in 1 mL of $CHCl_3$ was added to 25 µL of linoleic acid, and 200 mg of Tween 40 emulsifier in a bottle. After $CHCl_3$ evaporated, the mixture was dissolved using 100 mL of pure water saturated with singlet oxygen. Briefly, 160 µL of prepared reactive was mixed with 40 µL of **P1-P14** derivatives dissolved in DMSO at different concentrations. The zero-time absorbance was measured at 470 nm, and the measurement was done every 30 min up to the absorbance of control reduces under 0.1 absorbance in 96 well plate cell length.

3.1.5. In vitro Enzyme Inhibitory Activities

3.1.5.1. Determination of Anticholinesterase Activity of the P1-P14 Derivatives

The anti-ChE activity of **P1-P14** derivatives was evaluated against AChE (Type-VI-S, EC 3.1.1.7, 425.84 U/mg ve BChE (EC 3.1.1.8, 11.4 U/mg) assays using spectroscopic method [32, 36]. Acetylthiocholine iodide and butyryl-thiocholine chloride were employed as substrates. Briefly, 130 µL sodium phosphate buffer (100 mM, pH 8.0), 10 µL **P1-P14** derivatives at different concentrations, and 20 µL AChE or BChE enzymes in the buffer were mixed. After incubation for 15 min at 25°C , 20 µL 0.5 mM DTNB (5,5-dithiobis(2-nitrobenzoic acid) and 20 µL acetylthiocholine iodide (0.71 mM) or butyryl-thiocholine chloride (0.2 mM) were added. Then, the absorbance was pre/end measured at 412 nm. Galantamine was used as a positive standard to compare the AChE or BChE inhibitory activity of **P1-P14**.

3.1.5.2. Determination of Tyrosinase Inhibitory Activity of the P1-P14 Derivatives

The mushroom tyrosinase (EC 232-653-4, 250 KU) was used to determine the inhibitory activity of the **P1-P14** derivatives where L-DOPA was substrate according to DOPA chrome method [32, 37]. Briefly, 150 µL of 50 mM sodium phosphate buffer (pH 6.8), 10 µL of **P1-P14** derivatives in DMSO, and 20 µL of tyrosinase solution (13.3 U/well) were added in a 96-well plate. After 10 min incubation at 37 °C, L-DOPA (0.5 mM) was added to start the enzymatic reaction. The enzymatic reaction formation of DOPA chrome was monitored using 475 nm wavelength at 37 °C for 10 min. Kojic acid and L-mimosine were used as positive standards to compare the tyrosinase inhibitory activity of **P1-P14**.

3.1.5.3. Determination of α-amylase Inhibitory Activity of the P1-P14 Derivatives

α-Amylase inhibitory activity of the **P1-P14** derivatives was tested by using the spectroscopic method with slight changes [32, 38]. Briefly, 25 µL of **P1-P14** solution in different concentrations and 50 µL α-amylase solution (0.1 U/mL) in phosphate buffer (20 mM pH=6.9 phosphate buffer prepared with 6 mM NaCl) were added in a 96-well microplate. The mixture was pre-incubated for 10 min at 37°C . After pre-incubation, 50 µL starch solution (0.05%) was added and incubated for 10 min at 37°C . The reaction was stopped by the addition of 25 µL HCl (0.1 M) and then 100 µL Lugol solutions were added for monitoring. The 96-well microplate reader was taken to absorbance measure at 565 nm. Acarbose was

used as the positive standard to compare the α-amylase inhibitory activity of **P1-P14**.

3.1.5.4. Determination of α-glucosidase Inhibitory Activity of the P1-P14 Derivatives

α-Glucosidase inhibitory activity of the **P1-P14** derivatives was determined using the spectroscopic method with slight modifications [32, 39]. Briefly, 50 µL of phosphate buffer (10 mM pH=6.9), 25 µL of PNPG (*p*-nitrophenyl-*α-D*-glucopyranoside) in phosphate buffer (10 mM pH=6.9), 10 µL of **P1-P14** solution dissolved in DMSO at different concentrations and 25 µL of α-glucosidase (0.1 U/mL) in phosphate buffer (10 mM pH=6.0) were mixed in a 96-well microplate, respectively. After 20 min incubation at 37°C , 90 µL of Na_2CO_3 solution (100 mM) was added into each well to stop the enzymatic reaction. The absorbance of the 96-well microplate reader was recorded at 400 nm. Acarbose was used as the positive standard to compare the α-glucosidase inhibitory activity of **P1-P14**.

3.2. Molecular Docking Studies

A molecular docking simulation was carried out to investigate the interactions of compounds with two target enzymes. Firstly, the compounds were sketched in ChemDraw v.15 software, optimized using the MM2 method, and saved in pdb format, then their pdbqt formats were provided by AutoDock Tools v.1.5.7. On the other hand, experimentally determined crystal structures of the target enzymes α-amylase (PDB code: 1B2Y) and α-glucosidase (PDB code: 5PDB: 5NN8) were downloaded from the RSCB PDB databank (https://www.rcsb.org/). To prepare the target enzymes for docking simulation, heterogroups such as water, other ligands, and ions were first removed and their polar hydrogens, Kollman and Gasteiger charges were added to residues in the target structures using AutoDock Tools v.1.5.7. The binding sites of the target enzymes were determined by active residues and the coordinates for each target, the grid box was centered around the ligands inside enzymes with a grid spacing of 0.375 Å in each dimension and 50 × 50 × 50 grid points for each grid map. The Lamarckian Genetic Algorithm (LGA) [40] method was performed with 100 independent docking runs for each synthesized compound. The population size, maximum number of scores, and maximum number of generations were set to 150, 25,000,000, and 27,000, respectively. The maximum RMS tolerance was 2Å for conformational cluster analysis. At the end of the docking analysis, the estimated free energies of ligand binding (ΔG, kcal/mol) were calculated and interactions between target enzymes and ligands were visualized using Discovery Studio Visualizer v.21.

3.3. *In silico* ADME Studies

The SwissAdme web server was used to evaluate the physicochemical and druglikeness properties of the compounds (Access date: 01.08.2023). The BOILED-Egg graph, which shows the ability of compounds to pass through biological systems such as the blood-brain barrier and gastrointestinal membranes, was also obtained *via* this program. Mutagenicity, tumorigenicity, skin irritancy, reproductive effects and irritant risks were calculated on Osiris property Explorer (Access date: 01.08.2023).

CONCLUSION

The pyrazoline structures are frequently encountered in drug research and development studies due to their different biological activities. For this purpose, the synthesis of some novel compounds with 2-pyrazoline structure and the elucidation of their structures were carried out. In addition, different biological activities of these pyrazoline structures, such as antioxidant, anticholinesterase, antityrosinase and antidiabetic were investigated in this study. In the antioxidant activity screening of these compounds, **P14** showed more antioxidant activity in both $ABTS^{\cdot+}$ and β-carotene/linoleic acid assays than standard BHA. **P12** also showed significant antioxidant activity only in β-carotene/linoleic acid experiments. In enzyme activity studies of the compounds, **P1**, which has cyano and methoxy groups on the aromatic ring, showed approximately 1.5 times more inhibitory activity than acarbose against α-amylase. Furthermore, **P5**, which carries chlorine and cyano groups on the aromatic ring, showed approximately 20 times more inhibitory activity than acarbose against α-glucosidase. It is estimated that it is compatible with Lipinski and Veber rules, has high bioavailability and the risk of toxicity is low, especially for compounds containing the cyano group. The docking results showed a good correlation with the biological profile of **P1** and **P5** with the α-amylase and α-glucosidase. Compounds **P1** and **P5** could lead compounds for further studies against antidiabetic activity.

LIST OF ABBREVIATIONS

AChE = Acetylcholinesterase

BChE = Butyrylcholinesterase

MAO = Monoamine Oxidase

ADME = Absorption, Distribution, Metabolism and Excretion

CONSENT FOR PUBLICATION

Not applicable.

AVAILABILITY OF DATA AND MATERIALS

The data and supportive information are available within the article.

FUNDING

This work was partly supported by the TUBITAK (The Scientific and Technological Research Council of Turkey) with a Project Name: 2209-A Research Project Support Programme for Undergraduate Students (No: 1919B012201136 and 1919B012201137).

CONFLICT OF INTEREST

The authors declare no conflict of interest, financial or otherwise.

ACKNOWLEDGEMENTS

Declared none.

SUPPLEMENTARY MATERIAL

Supplementary material is available on the publisher's website along with the published article.

REFERENCES

[1] Yan, R.; Huang, X.; Deng, X.; Song, M. Synthesis and activity evaluation of some pyrazole–pyrazoline derivatives as dual Anti-inflammatory and antimicrobial agents. *Polycycl. Aromat. Compd.,* **2022**, *42*(8), 5006-5019. http://dx.doi.org/10.1080/10406638.2021.1919156

[2] Turan-Zitouni, G.; Özdemir, A.; Kaplancikli, Z.A.; Chevallet, P.; Tunali, Y. Synthesis and antimicrobial activities of some 1-[(N, N-disubstitutedthiocarbamoylthio)acetyl]-3,5-diaryl-2-pyrazolines. *Phosphorus Sulfur Silicon Relat. Elem.,* **2005**, *180*(12), 2717-2724. http://dx.doi.org/10.1080/104265090930452

[3] Acar Çevik, U.; Osmaniye, D.; Sağlik, B.N.; Levent, S.; Kaya Çavuşoğlu, B.; Özkay, Y.; Kaplancikli, Z.A. Synthesis and evaluation of new pyrazoline-thiazole derivatives as monoamine oxidase inhibitors. *J. Heterocycl. Chem.,* **2019**, *56*(11), 3000-3007. http://dx.doi.org/10.1002/jhet.3694

[4] Kaplancıklı, Z.A.; Özdemir, A.; Turan-Zitouni, G.; Altıntop, M.D.; Can, Ö.D. New pyrazoline derivatives and their antidepressant activity. *Eur. J. Med. Chem.,* **2010**, *45*(9), 4383-4387. http://dx.doi.org/10.1016/j.ejmech.2010.06.011 PMID: 20587366

[5] Özkay, Ü.D.; Can, Ö.D.; Kaplancıklı, Z.A. Antinociceptive activities of some triazole and pyrazoline moieties-bearing compounds. *Med. Chem. Res.,* **2012**, *21*(7), 1056-1061. http://dx.doi.org/10.1007/s00044-011-9619-z

[6] Asad, M.; Khan, S.A.; Arshad, M.N.; Asiri, A.M.; Rehan, M. Design and synthesis of novel pyrazoline derivatives for their spectroscopic, single crystal X-ray and biological studies. *J. Mol. Struct.,* **2021**, *1234*, 130131. http://dx.doi.org/10.1016/j.molstruc.2021.130131

[7] Aqlan, F.M. Synthesis characterization and *in vitro* antibacterial activity of the N-substituted bis-pyrazoline derivative as polycyclic aromatic compounds. *Polycycl. Aromat. Compd.,* **2022**, *42*(6), 3412-3421. http://dx.doi.org/10.1080/10406638.2020.1866040

[8] Sharma, K.; Kumar, A.; Prakash, R.; Tripathi, A.; Singh, R.; Bajpai, R.; Sahasrabuddhe, A.A.; Singh, D.; Narender, T. Pyrazoline analogues: Design, synthesis, and evaluation of anti-osteoporosis activity. *Bioorg. Med. Chem. Lett.,* **2022**, *60*, 128585. http://dx.doi.org/10.1016/j.bmcl.2022.128585 PMID: 35085723

[9] Ashraf, S.; Hameed, S.; Tahir, M.N.; Naseer, M.M. Synthesis and crystal structure of bis-chalcone-derived fused-ring pyrazoline having an unusual substitution pattern. *Monatsh. Chem.,* **2017**, *148*(10), 1871-1875. http://dx.doi.org/10.1007/s00706-017-1995-8

[10] Salih, R.H.H.; Hasan, A.H.; Hussen, N.H.; Hawaiz, F.E.; Hadda, T.B.; Jamalis, J.; Almalki, F.A.; Adeyinka, A.S.; Coetzee, L.C.C.; Oyebamiji, A.K. Thiazole-pyrazoline hybrids as potential antimicrobial agent: Synthesis, biological evaluation, molecular docking, DFT studies and POM analysis. *J. Mol. Struct.,* **2023**, *1282*, 135191. http://dx.doi.org/10.1016/j.molstruc.2023.135191

[11] Matiadis, D. Strategies and methods for the synthesis of 2-pyrazolines: Recent developments (2012–2022). *Adv. Synth. Catal.,* **2023**, *365*(12), 1934-1969. http://dx.doi.org/10.1002/adsc.202300373

[12] Tok, F.; Koçyiğit-Kaymakçıoğlu, B.; Sağlık, B.N.; Levent, S.; Özkay, Y.; Kaplancıklı, Z.A. Synthesis and biological evaluation of new pyrazolone Schiff bases as monoamine oxidase and cholinesterase inhibitors. *Bioorg. Chem.,* **2019**, *84*, 41-50. http://dx.doi.org/10.1016/j.bioorg.2018.11.016 PMID: 30481645

[13] Tok, F.; Baltaş, N.; Tatar, G.; Koçyiğit-Kaymakçıoğlu, B. Synthesis, biological evaluation and *in silico* studies of new pyrazoline derivatives bearing benzo[d]thiazol-2(3H)-one moiety as potential urease inhibitors. *Chem. Biodivers.,* **2022**, *19*(3), e202100826. http://dx.doi.org/10.1002/cbdv.202100826 PMID: 35018718

[14] Tok, F.; Erdoğan, Ö.; Çevik, Ö.; Koçyiğit-Kaymakçıoğlu, B. Design, synthesis, *in silico* ADMET studies and anticancer activity of some new pyrazoline and benzodioxole derivatives. *Acta Chim. Slov.,* **2022**, *69*(2), 293-303. http://dx.doi.org/10.17344/acsi.2021.7119 PMID: 35861084

[15] Maleki, B.; Azarifar, D.; Moghaddam, K.; Hojati, F.; Gholizadeh, M.; Salehabadi, H. Synthesis and characterization of a series of 1,3,5-trisubstituted-2-pyrazolines derivatives using methanoic acid under thermal condition. *J. Serb. Chem. Soc.,* **2009**, *74*(12), 1371-1376. http://dx.doi.org/10.2298/JSC0912371M

[16] Acharya, A.P.; Gaikwad, M.V.; Dawane, B.S. Synthesis, biological evaluations and molecular docking of novel pyrazolyl, dihydro-1H-inden-1-one derivatives. *Chem. Methodol,* **2022**, *6*(4), 339-346. http://dx.doi.org/10.22034/CHEMM.2022.329102.1441

[17] Azarifar, D.; Maleki, B. Silica-supported synthesis of some 1,3,5-trisubstituted 2-pyrazolines under solvent-free and microwave irradiation conditions. *J. Heterocycl. Chem.,* **2005**, *42*(1), 157-159. http://dx.doi.org/10.1002/jhet.5570420125

[18] Al-Shammari, W.A.M.; Lateef, S.M. Structural, spectroscopic, thermal, and biological studies of new Schiff base ligand derived from anthrone and 3-amino-1-phenyl-2-pyrazoline-5-one and its complexes with metallic Ions. *Chem. Methodol,* **2023**, *7*(8), 637-649.

[19] Morris, G.M.; Huey, R.; Lindstrom, W.; Sanner, M.F.; Belew, R.K.; Goodsell, D.S.; Olson, A.J. AutoDock4 and autodocktools4: Automated docking with selective receptor flexibility. *J. Comput. Chem.,* **2009**, *30*(16), 2785-2791. http://dx.doi.org/10.1002/jcc.21256 PMID: 19399780

[20] Can, N.; Çevik, U.A.; Sağlık, B.N.; Özkay, Y.; Atlı, Ö.; Baysal, M.; Özkay, Ü.D.; Can, Ö.D. Pharmacological and toxicological screening of novel benzimidazole-morpholine derivatives as dual-acting inhibitors. *Molecules,* **2017**, *22*(8), 1374. http://dx.doi.org/10.3390/molecules22081374 PMID: 28825626

[21] Kurşun Aktar, B.S.; Sıcak, Y.; Tok, T.T.; Oruç-Emre, E.E.; Yağlıoğlu, A.Ş.; Iyidoğan, A.K.; Öztürk, M.; Demirtaş, I. Designing heterocyclic chalcones, benzoyl/sulfonyl hydrazones: An insight into their biological activities and molecular docking study. *J. Mol. Struct.,* **2020**, *1211*, 128059. http://dx.doi.org/10.1016/j.molstruc.2020.128059

[22] Akdağ, K.; Tok, F.; Karakuş, S.; Erdoğan, Ö.; Çevik, Ö.; Kaymakçıoğlu, B. Synthesis and biological evaluation of some hydrazide-hydrazone derivatives as anticancer agents. *Acta Chim. Slov.,* **2022**, *69*(4), 863-875. http://dx.doi.org/10.17344/acsi.2022.7614 PMID: 36562164

[23] Azman, M.; Sabri, A.H.; Anjani, Q.K.; Mustaffa, M.F.; Hamid, K.A. Intestinal absorption study: Challenges and absorption enhancement strategies in improving oral drug delivery. *Pharmaceuticals,* **2022**, *15*(8), 975. http://dx.doi.org/10.3390/ph15080975 PMID: 36015123

[24] Karaca Gençer, H.; Acar Çevik, U.; Levent, S.; Sağlık, B.; Korkut, B.; Özkay, Y.; Ilgın, S.; Öztürk, Y. New benzimidazole-1,2,4-triazole hybrid compounds: Synthesis, anticandidal activity and cytotoxicity evaluation. *Molecules,* **2017**, *22*(4), 507. http://dx.doi.org/10.3390/molecules22040507 PMID: 28346364

[25] Tok, F.; Doğan, M.O.; Gürbüz, B.; Koçyiğitkaymakçioğlu, B. Synthesis of novel pyrazoline derivatives and evaluation of their antimicrobial activity. *J. Res. Pharm.,* **2022**, *26*(5), 1453-1460. http://dx.doi.org/10.29228/jrp.238

[26] Tok, F.; Koçyiğit-Kaymakçıoğlu, B. Design, synthesis and biological screening of novel 1,5-diphenyl-3-(4-(trifluoromethyl)phenyl)-2-pyrazoline derivatives. *Acta Chim. Slov.,* **2020**, *67*(4), 1139-1147. http://dx.doi.org/10.17344/acsi.2020.6028 PMID: 33533467

[27] Wang, Y.; Rivera Vera, C.I.; Lin, Q. Convenient synthesis of highly functionalized pyrazolines *via* mild, photoactivated 1,3-dipolar cycloaddition. *Org. Lett.,* **2007**, *9*(21), 4155-4158. http://dx.doi.org/10.1021/ol7017328 PMID: 17867694

[28] Miura, T.; Hagiwara, K.; Nakamuro, T.; Nagata, Y.; Oku, N.; Murakami, M. Regioselective 1,3-dipolar cycloaddition of nitriles with nitrile imines generated from tetrazoles. *Chem. Lett.,* **2021**, *50*(1), 131-135. http://dx.doi.org/10.1246/cl.200634

[29] Ghorbani, P.; Nasr-Esfahani, M.; Eftekhari Far, B. Synthesis of chalcones and pyrazolines using NB-Fe_3O_4@SiO_2@CPTMO@DEA-SO_3H as an efficient and reusable nanocatalyst. *Russ. J. Org. Chem.,* **2022**, *58*(12), 1812-1820. http://dx.doi.org/10.1134/S1070428022120107

[30] Re, R.; Pellegrini, N.; Proteggente, A.; Pannala, A.; Yang, M.; Rice-Evans, C. Antioxidant activity applying an improved ABTS radical cation decolorization assay. *Free Radic. Biol. Med.,* **1999**, *26*(9-10), 1231-1237. http://dx.doi.org/10.1016/S0891-5849(98)00315-3 PMID: 10381194

[31] Sıcak, Y.; Şahin-Yağlıoğlu, A.; Öztürk, M. Bioactivities and phenolic constituents relationship of Muğla thyme and pine honey of Turkey with the chemometric approach. *J. Food Meas. Charact.,* **2021**, *15*(4), 3694-3707. http://dx.doi.org/10.1007/s11694-021-00940-8

[32] Tok, F.; Çakir, C.; Çam, D.; Kirpat, M.M.; Sicak, Y. Synthesis, characterization and biological evaluation of novel thiourea derivatives. *Clin. Exp. Health Sci.,* **2022**, *12*(2), 533-540. http://dx.doi.org/10.33808/clinexphealthsci.1062872

[33] Blois, M.S. Antioxidant determinations by the use of a stable free radical. *Nature,* **1958**, *181*(4617), 1199-1200. http://dx.doi.org/10.1038/1811199a0

[34] Apak, R.; Güçlü, K.; Özyürek, M.; Karademir, S.E. Novel total antioxidant capacity index for dietary polyphenols and vitamins C and E, using their cupric ion reducing capability in the presence of neocuproine: CUPRAC method. *J. Agric. Food Chem.,* **2004**, *52*(26), 7970-7981. http://dx.doi.org/10.1021/jf048741x PMID: 15612784

[35] Marco, G.J. A rapid method for evaluation of antioxidants. *J. Am. Oil Chem. Soc.,* **1968**, *45*(9), 594-598. http://dx.doi.org/10.1007/BF02668958

[36] Ellman, G.L.; Courtney, K.D.; Andres, V., Jr; Featherstone, R.M. A new and rapid colorimetric determination of acetylcholinesterase activity. *Biochem. Pharmacol.,* **1961**, *7*(2), 88-95. http://dx.doi.org/10.1016/0006-2952(61)90145-9 PMID: 13726518

[37] Hearing, V.J. *Methods in enzymology*; Academic Press: NewYork, **1987**, 142, pp. 154-165.

[38] Quan, N.; Xuan, T.; Tran, H.D.; Thuy, N.; Trang, L.; Huong, C.; Andriana, Y.; Tuyen, P. Antioxidant, α-amylase and α-glucosidase inhibitory activities and potential constituents of canarium tramdenum bark. *Molecules,* **2019**, *24*(3), 605. http://dx.doi.org/10.3390/molecules24030605 PMID: 30744084

[39] Kim, J.S.; Kwon, C.S.; Son, K.H. Inhibition of alpha-glucosidase and amylase by luteolin, a flavonoid. *Biosci. Biotechnol. Biochem.,* **2000**, *64*(11), 2458-2461. http://dx.doi.org/10.1271/bbb.64.2458 PMID: 11193416

[40] Morris, G.M.; Goodsell, D.S.; Halliday, R.S.; Huey, R.; Hart, W.E.; Belew, R.K.; Olson, A.J. Automated docking using a Lamarckian genetic algorithm and an empirical binding free energy function. *J. Comput. Chem.,* **1998**, *19*(14), 1639-1662. http://dx.doi.org/10.1002/(SICI)1096-987X(19981115)19:14<1639::AID-JCC10>3.0.CO;2-B